

## REPORT DOCUMENTATION PAGE

AFOSR-TR-97

Public reporting burden for this collection of information is estimated to average 1 hour per response, including the time for reviewing existing data, gathering new data, maintaining the data needed, and completing and reviewing the collection of information. Send comment regarding this burden estimate or any other aspect of this collection of information, including suggestions for reducing this burden, to Washington Headquarters Services, Directorate for Information Operations and Reports, 1215 Jefferson Davis Highway, Suite 1204, Arlington, VA 22202-4302, and to the Office of Management and Budget, Paperwork Reduction Project (0704-0188), Washington, DC 20503

0527

1. AGENCY USE ONLY (Leave blank)		2. REPORT DATE 3 October 1997		3. REPORT TYPE AND DATES COVERED Final Technical Report 1 July 94 - 30 June 97	
4. TITLE AND SUBTITLE High Pressure Combustion Studies Under Combustion Driven Oscillatory Flow Conditions				5. FUNDING NUMBERS PE - 61102F PR - 2308	
6. AUTHORS Robert J. Santoro				SA - AS G - F49620-94-1-0235	
7. PERFORMING ORGANIZATION NAME(S) AND ADDRESS(ES)  The Pennsylvania State University 240 Research Building East University Park, PA 16802				8. PERFORMING ORGANIZATION REPORT NUMBER	
9. SPONSORING / MONITORING AGENCY NAME(S) AND ADDRESS(ES)  AFOSR/NA 110 Duncan Avenue, Suite 115 Bolling AFB, DC 20332-0001				10. SPONSORING / MONITORING AGENCY REPORT NUMBER	
11. SUPPLEMENTARY NOTES					
12 a. DISTRIBUTION / AVAILABILITY STATEMENT  Approved for public release; distribution is unlimited					
12 b. DISTRIBUTION CODE					
13. ABSTRACT (Maximum 200 words)  Rocket engines fueled by a dense propellant such as kerosene provide a number of advantages over hydrogen-fueled engines for primary stages. A major problem in the development of liquid fueled rocket engines has been the occurrence of combustion instability. The lack of a detailed understanding of how combustion instability occurs in liquid-fueled rocket engines has resulted in costly engine development programs that must be avoided in the future. The present research program examined the specific effects of atomization in combustion instability. The effects of mean drop size, drop size distribution, and atomization periodicity were examined explicitly with a combustion response model, the results from which indicated that all of these effects were important. It was shown that periodic atomization, in particular, results in large variations in the magnitude of the response when the atomization frequency is on the same order as the acoustic oscillation frequency. Experimental results from a sub-scale rocket combustor that used electro-mechanically forced atomization to accentuate the natural frequency of periodic atomization associated with impinging jet injectors were also undertaken. The presence of forced longitudinal modes, corresponding to the forced atomization frequencies, substantiate the importance of periodic atomization. A conceptual model of this potentially dominant mechanism of combustion instability was also developed as part of the study.					
14. SUBJECT TERMS Combustion Instability, Impinging Jets, Rocket engines, combustion, atomization				15. NUMBER OF PAGES 30	
				16. PRICE CODE	
17. SECURITY CLASSIFICATION OF REPORT  UNCLASSIFIED		18. SECURITY CLASSIFICATION OF THIS PAGE  UNCLASSIFIED		19. SECURITY CLASSIFICATION OF ABSTRACT  UNCLASSIFIED	
20. LIMITATION OF ABSTRACT  UL					

19971021 174

DO NOT QUOTE IN ABSTRACT

Final Report  
on  
**High Pressure Combustion Studies Under Combustion-Driven  
Oscillatory Flow Conditions**

for  
AFOSR Contract/Grant F49620-94-1-0235

Prepared by

Robert J. Santoro  
Propulsion Engineering Research Center  
and  
Department of Mechanical Engineering  
The Pennsylvania State University  
University Park, PA 16802

Submitted to:

Air Force Office of Scientific Research  
Bolling Air Force Base  
Washington D.C.

October 1997

## TABLE OF CONTENTS

1.0	RESEARCH OBJECTIVE.....	1
2.0	ANALYTICAL RESULTS.....	3
3.0	EXPERIMENTAL RESULTS.....	12
4.0	SUMMARY.....	20
5.0	REFERENCES.....	22
6.0	PUBLICATIONS.....	24
7.0	PARTICIPATING PROFESSIONALS.....	25
8.0	MEETINGS AND PRESENTATIONS .....	26
9.0	INTERACTIONS.....	27

## 1.0 RESEARCH OBJECTIVE

For many launch applications the use of liquid (non-cryogenic) fuel is desirable. Liquid fuels are much denser than hydrogen and easier to handle. These attributes are particularly advantageous for the first stage of a multiple-stage low-cost system, for instance, or for launch-on-demand applications. A major issue in the development of liquid-fueled rocket engines, as compared to engines using cryogenic fuels, is whether the combustor can be made free from combustion-generated pressure oscillations that could lead to catastrophic failure.

The initiation and growth of these pressure oscillations, commonly referred to as combustion instabilities, are primarily determined by the design of the injector. A good injector design provides oscillation-free operation throughout the operating envelope and acceptable thrust efficiency. Historically, rocket engines fueled by liquid hydrocarbons have had thrust efficiencies on the order of three to five percent less than their hydrogen-fueled counterparts [1]; this is not because design strategies for efficient combustors are unknown, but rather because the design strategies that lead to very efficient combustion also tend to promote the occurrence of high-frequency combustion instability in liquid-fueled rocket engines.

Instabilities can be classified according to whether they occur as bulk mode oscillations or in resonance with the chamber's acoustic modes, and by the mechanisms by which they are initiated and amplified [2]. Pressure oscillations which are due to fluctuations in the propellant flow rate are referred to as injection-coupled instabilities. Injection-coupled instabilities are amplified when the flow rate oscillations become coupled with either bulk- or acoustic-mode chamber pressure oscillations. Eliminating injection-coupled instabilities (chug instabilities) is accomplished by increasing the injection pressure drop (by reducing the injection flow area, or by increasing the propellant flowrate). Acoustic mode instabilities, which occur at a higher frequency than chug instabilities, can also be due to injection-coupling. Longitudinal-mode instabilities are usually injection-coupled, and are acoustic in nature with a pressure antinode at the injector face. Injection-coupled instabilities are well-modeled with conventional time lag models and are relatively easy to avoid or eliminate.

More problematic than the injection-coupled instabilities are the instabilities that are intrinsically coupled to the combustion processes. These intrinsic instabilities typically occur when the energy release density in the combustor is increased; as the energy release density increases, higher modes of combustion instability occur. To eliminate these instabilities, the

injection pressure drop is reduced or the injector element orifice size is enlarged, both of which tend to decrease energy release density and combustion efficiency in a fixed volume combustor. This purposeful decrement of performance to achieve combustion stability is the reason that liquid-fueled rocket engines operate with a lower combustion efficiency than do hydrogen-fueled rocket engines.

To develop effective design strategies for the elimination or control of combustion instabilities and to realize the benefits of liquid-fueled rocket engines, it is necessary to define the physical mechanisms that lead to the growth of these instabilities. Most of the work to date on combustion instability mechanisms has been based on the premise that intrinsic instabilities are controlled by vaporization. This premise is based explicitly on the proposition that vaporization is the rate-limiting step in spray combustion, and implicitly on the proposition that the sensitive time lag theory [3] holds for intrinsic-type instabilities. The role of atomization was dismissed largely on the basis that it occurred at a very high rate.

The work carried out under this program presents evidence to support the hypothesis that the atomization process, especially that associated with impinging jet injectors, is the key factor in determining whether intrinsic instabilities will occur in liquid-fueled combustors. Previous work conducted in our laboratory under an earlier AFOSR grant emphasized measurements of a cold-flow spray formed by impinging jet injectors, which are commonly used with liquid fuels [4]. The measurements included atomization frequency and drop size distribution. The experimental results were compared with an empirical stability correlation used to predict the highest sustainable frequency of combustion instability in rocket engines that use impinging jet injectors to shed light on the physical basis of the correlation [5,6]. It was found that atomization is a periodic phenomenon that occurs on a time scale remarkably similar to typical combustion instabilities. Furthermore, the atomization frequency increases linearly with the ratio of injection velocity-to-orifice diameter ( $U_j/d_o$ ), as does the highest frequency of combustion instability predicted by the empirical correlation, which is essentially of the form  $f_{inst}d_o/U_j \sim 0.1$ . As an increasing tendency toward combustion instability was predicted by the correlation, the measurements indicated that the average drop size and the polydispersity of the drop size distribution both decreased.

Under the current program, experiments and analyses were conducted to further examine the connection between atomization and combustion instability.

## 2.0 ANALYTICAL RESULTS

The combustion response methodology is a standard approach for analyzing combustion stability [7]. In this analysis, the changes in combustion rate due to ambient oscillations are calculated and integrated to determine the amount of the heat release that occurs in phase with the pressure oscillation. A large positive value of combustion response indicates that a strong potential for a coupling between acoustic oscillations and heat release exists, and that combustion instability may occur. If vaporization is assumed to be the rate-limiting step in combustion, then the combustion response may be approximated by the vaporization response.

The in-phase response factor,  $R$ , is defined as:

$$R = \frac{\int_0^{t_{drop}} m' p' dt}{\int_0^{t_{drop}} (p')^2 dt} \quad (1)$$

where  $t_{drop}$  is the drop lifetime,  $m'$  is the unsteady component of the vaporization rate, and  $p'$  is the unsteady component of the ambient pressure. In the present implementation of the combustion response analysis, an open loop response is calculated. Theoretically, a value of  $R$  of at least  $(\gamma+1)/2\gamma \sim 0.9$  is required to drive a longitudinal instability for the case of concentrated combustion at the pressure antinode of a closed chamber, where  $\gamma$  is the specific heat ratio of the gas [3]. In the present analysis, the Priem-Heidmann model is used to calculate the vaporization rate [8].

A standing acoustic wave in a two-dimensional chamber was considered in the analysis, thus the pressure oscillates in a sinusoidal fashion:

$$p' \propto \cos(\omega t) \quad (2)$$

The pressure oscillations are accompanied by out-of-phase transverse velocity oscillations:

$$v_{trans} \propto \sin(\omega t) \quad (3)$$

The maximum amplitude of the pressure oscillation was set at 0.1 times the mean chamber pressure. The order of the amplitude of the transverse velocity oscillation associated with a pressure oscillation of  $p'$  is  $(a/\gamma)p'$ . This condition corresponds to a location in the chamber that is intermediate between a pressure antinode and a pressure node, where both oscillations in velocity and pressure are present.

The combustion response analysis is a straightforward and mechanistic means of predicting combustion stability characteristics. Accurate accounting of the combustion processes

is the main difficulty. Of all the component combustion processes, atomization is possibly the most difficult to model accurately. Most applications of the combustion response analysis greatly simplify the atomization process. Typically, an array of drops, all of the same size, is used to represent the actual distribution of drop sizes and velocities. The representative drop is "injected" continuously over one cycle of the pressure oscillation. These injection rates range from about 16 to 36 times per cycle [7,9]. Thus, the effects of unsteady atomization and drop size distribution are both precluded from the analysis.

The simplified version of atomization used in prior applications of the combustion response model results in a misinterpretation of some of the dominating aspects of combustion instability. Measurements associated with impinging jet injectors have shown that the frequency of atomization and combustion instability are actually quite similar [5]. A phenomenological model of atomization for impinging jet injectors was developed earlier [10]. The highest atomization frequency predicted by this model is shown in Fig. 1, and compared to results from an empirical correlation that predicts the highest frequency of combustion instability that can be driven by a given impinging jet injector design, and which has the form  $f_{inst} d_o / U_j \sim 0.1$ . It is seen that the highest instability frequency is about ten times less than the highest atomization frequency. Thus, in a combustion response model, it is incorrect to assume that atomization

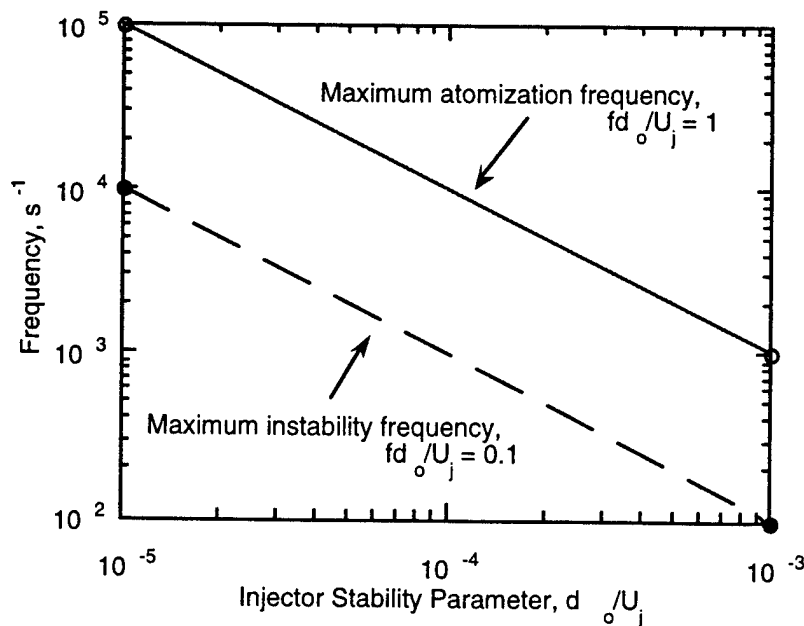


Fig. 1. A comparison between the maximum atomization frequencies associated with impinging jet injectors and combustion instability, as predicted by a phenomenological atomization model and the empirical stability correlation, respectively.

**Table 1. Study Cases Used in Response Analysis of Heptane/Oxygen Combustion**

Case Number	$d_o/U_j$ , $s \times 10^5$	High-frequency cutoff, $s^{-1}$	Atomization frequency, $s^{-1}$	$d_{10}$ , $\mu m$	$d_{32}$ , $\mu m$
1	2.59	3861	15,914	110	372
2	3.43	2915	11,529	133	389
3	4.10	2439	9391	154	455
4	5.12	1953	7272	182	472
5	9.98	1002	3365	383	576

occurs continuously over a pressure oscillation cycle. This point will be shown to have a major impact on the magnitude of combustion response below. The fact that the atomization frequency is linearly dependent on the stability parameter, as is the highest sustainable frequency of combustion instability, suggests a strong coupling mechanism between unsteady atomization and combustion instability.

The combustion response analysis used here considers heptane drops burning in an oxygen environment. The measured size distribution for a water spray formed by impinging jets was converted to a heptane spray size distribution by accounting for the property differences of ambient gas density, liquid density, and surface tension by using the following correlation [11]:

$$d_d \propto \sigma^{0.16} \left( \frac{\rho_l}{\rho_g} \right)^{0.1} \quad (4)$$

The ambient pressure chosen for the study was 1.72 MPa (250 psia), which is approximately the nominal design pressure of the combusting-flow tests that proceeded in parallel. The molecular weight of the products of heptane-oxygen combustion is 30 kg/kmole and the ambient gas temperature was chosen to be 3500 K. The resultant heptane drop size distribution is shown in Fig. 2. Table 1 provides a summary of the cases considered in the combustion response analysis at the conditions employed in the analysis, including the atomization frequency as calculated from an atomization model developed earlier [10].



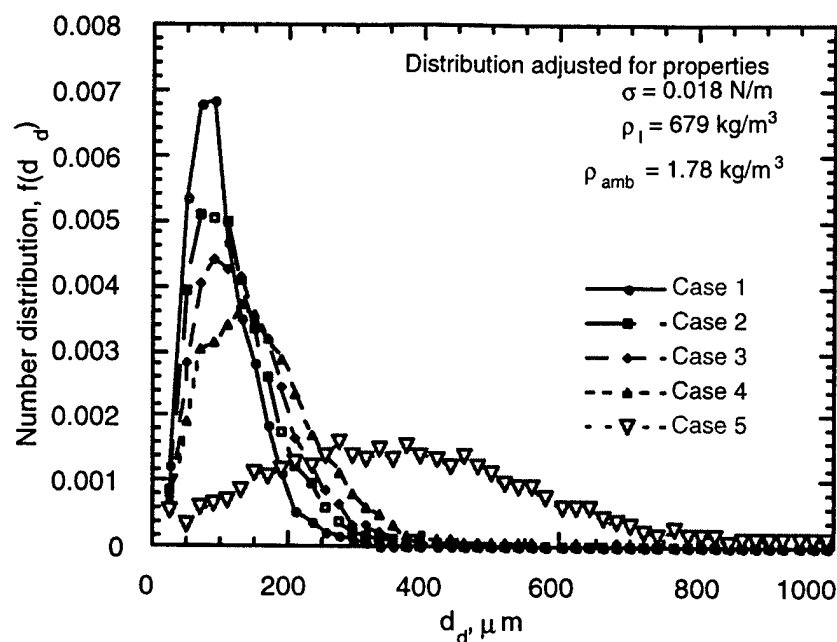


**Fig. 2.** The number distribution of heptane drops used in the combustion response analysis. The distribution was based on measured water spray and adjusted for property differences.

The vaporization rates of the drops under non-oscillatory conditions are shown in Fig. 3. The rates are normalized by the initial mass of the drop,  $m_0$ . The smallest mean-size drops

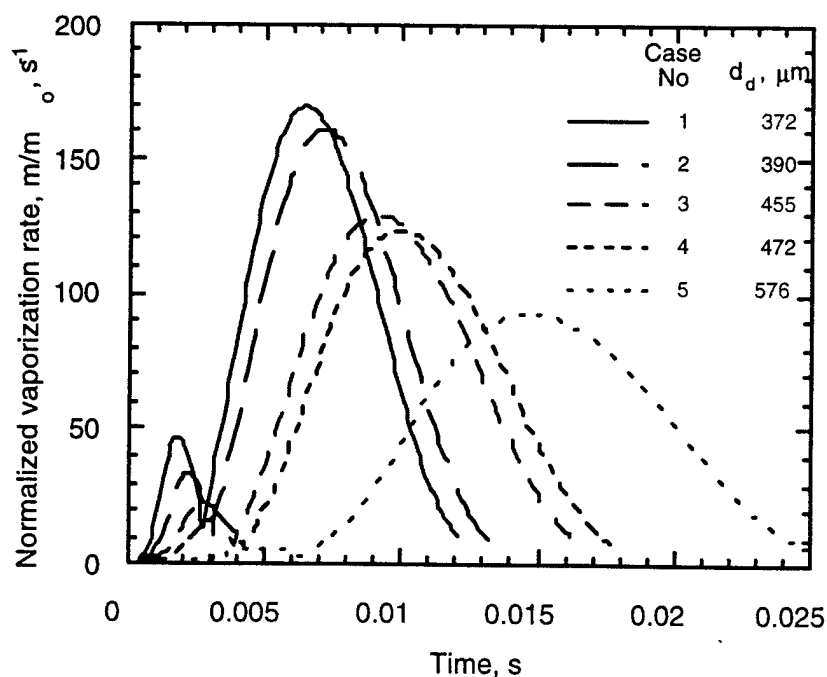


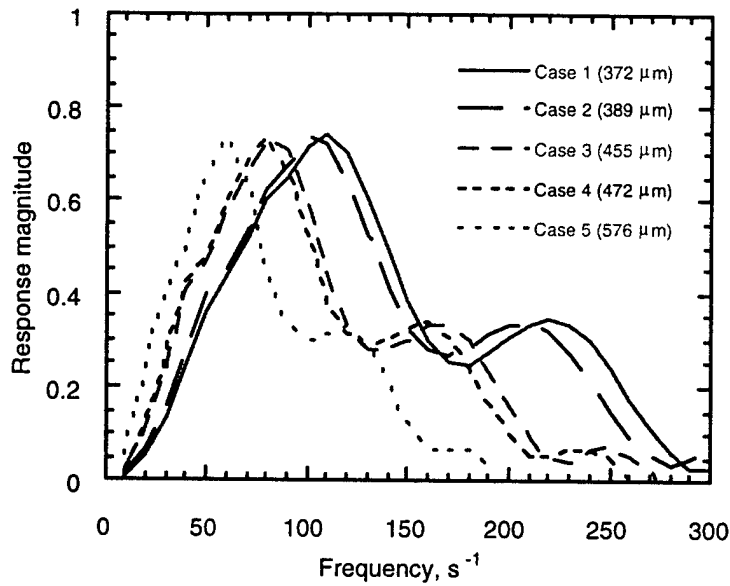
**Fig. 3.** The normalized vaporization rate of a heptane drop.

(Case 1,  $d_{32} \sim 370 \mu\text{m}$ ) vaporize within 12 ms, whereas the largest drops (Case 5,  $d_{32} \sim 575 \mu\text{m}$ ) take about 25 ms to vaporize. The drop undergoes a regime where the difference between its velocity and the ambient gas velocity is a minimum, and this regime is indicated most clearly by the local minima in the vaporization rate. This regime, which occurs at about three milliseconds for the smallest drop (Case 1) and at about six milliseconds for the largest drop (Case 5), is the regime which Priem and Guentert regarded as being most unstable because here the drops are most susceptible to transverse velocity oscillations associated with the unsteady flowfield [12].

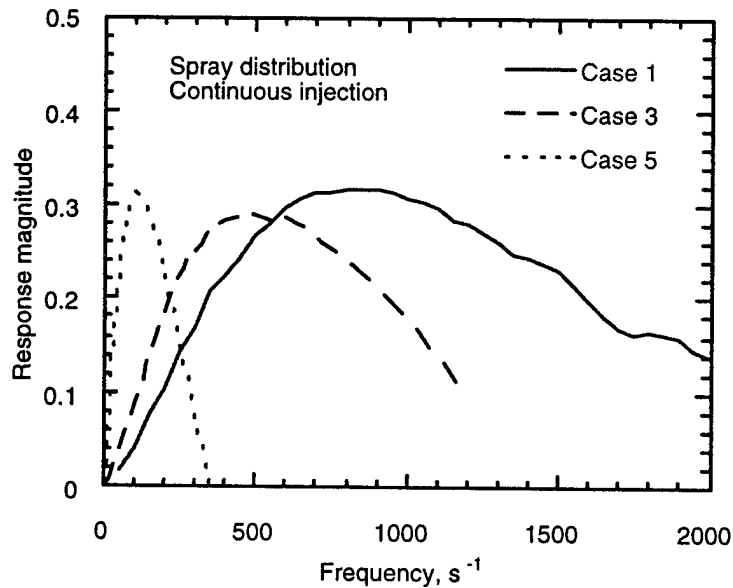
Three different approaches were used to calculate vaporization response. The first approach is conventional and uses a mean drop size ( $d_{32}$ ) to represent the spray. The continuous atomization approximation is used. For the second approach, the distribution of heptane drops shown in Fig. 2 is injected continuously over the period of oscillation. For both approaches using continuous atomization, the time interval between each injection was 1/16 of the period of oscillation, which is the value recommended in the ROCCID code [13]. Each of these approaches also uses the experimental data from Table 1 and Fig. 2 as input to the model. Since the drop size is dependent on the atomization frequency, it is difficult to decouple the effects of drop size and atomization frequency. Thus, the third approach is a parametric study of the effects of unsteady atomization on the combustion response of a single drop of a given size.

Figure 4 shows the vaporization response of continuously atomized drops with a diameter equal to the Sauter mean diameter ( $d_{32}$ ) of the distribution. The frequency at which the peak response occurs is inversely proportional to drop size, and ranges from about  $60 \text{ s}^{-1}$  for the  $576 \mu\text{m}$  drop to about  $110 \text{ s}^{-1}$  for the  $372 \mu\text{m}$  drop. The peak response is essentially independent of frequency, and is about 0.75. These results are consistent with many of the response calculations reported previously which indicated response magnitudes too low to drive an instability [7,9,14]. The frequencies corresponding to the predicted peak response magnitude are much lower than the high-frequency cutoff values indicated in Table 1.

Figure 5 shows the vaporization response for the continuously atomized distribution of drops. The peak vaporization responses are attenuated by about 50% as compared to those of the continuously atomized mean drop sizes. For Case 1, the case with the smallest mean diameter and the least disperse distribution, the peak response is 0.32 and occurs at a frequency of about  $900 \text{ s}^{-1}$ . The peak response magnitude for Case 5, having the largest mean drop size and the most disperse distribution, is 0.31 at a frequency of about  $100 \text{ s}^{-1}$ . The magnitude of the response is



**Fig. 4. Vaporization response magnitude of mean-sized drops as a function of ambient acoustic oscillation frequency.**



**Fig. 5. Vaporization response magnitude of heptane drops with the distribution shown in Fig. 2. Drops are added to the combustion zone continuously.**

insufficient to drive an instability for either the  $d_{32}$ -based or the distribution-based method. The use of the drop size distribution rather than the mean drop size also has an effect on the width of the response.

A comparison of the peak response frequencies predicted by the combustion response model with the high-frequency cutoff predicted by the empirical stability correlation (see Table 1) reveals that either application of the response analysis tends to underpredict the most

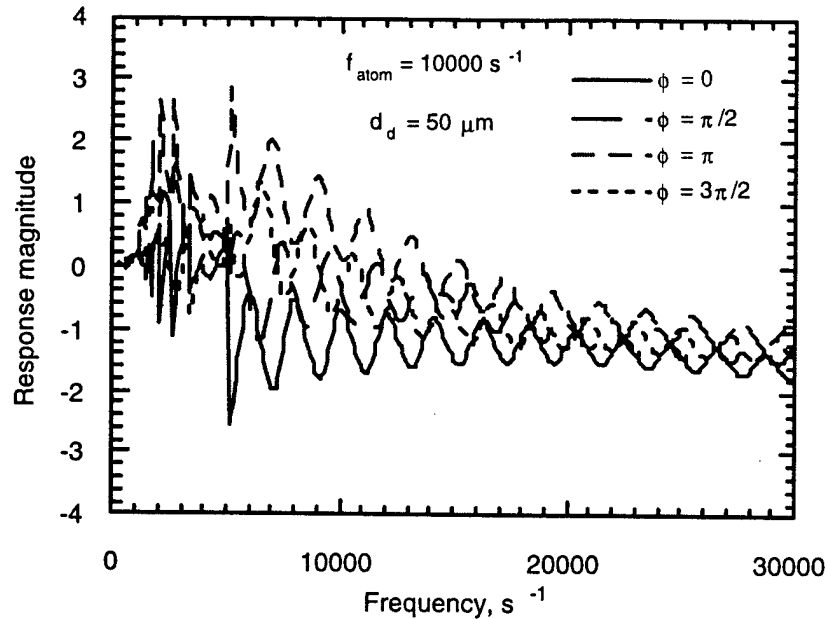


**Fig. 6. Vaporization response magnitude as a function of pressure oscillation frequency and phase angle  $\phi$ . Injection velocity was 20 m/s and ambient gas temperature was 3500 K. Atomization frequency was  $10,000 \text{ s}^{-1}$ .**

amplified frequency. It is important to note that the empirical stability correlation does not necessarily predict the frequency with the highest growth rate; rather, it predicts the highest frequency of instability that is observed in practical combustors.

Calculations were also done where the atomization frequency of Table 1 was used in conjunction with the drop size distribution of Fig. 2. This is a more realistic case than was considered in either of the prior two approaches. The calculated combustion response magnitudes for the unsteady atomization core were significantly larger than for the case of drop size distribution with continuous atomization. The combustion response magnitude was also dependent on the phase angle,  $\phi$ , between the pressure oscillation and the onset of unsteady atomization. A parametric study of the effects of unsteady atomization was performed since the exact relationship between atomization and the pressure oscillations can only be assumed. Drops with diameters ranging from  $10 \text{ } \mu\text{m}$  to  $100 \text{ } \mu\text{m}$  and atomization frequencies ranging from  $5000 \text{ s}^{-1}$  to  $15,000 \text{ s}^{-1}$  were varied independently to evaluate their effects on the response function.

Representative results of the calculated response magnitude as a function of acoustic oscillation frequency and phase angle are shown in Fig. 6 for the  $50 \text{ } \mu\text{m}$  drop size case. For this case, the atomization frequency was  $10,000 \text{ s}^{-1}$ . For all the cases with unsteady atomization, the

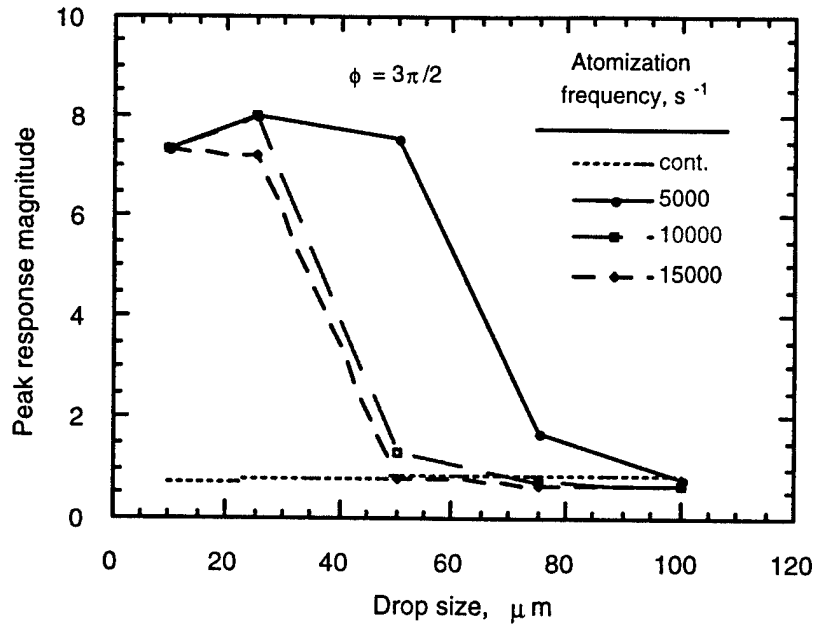


**Fig. 7. Peak response magnitude as a function of drop size and atomization frequency for a constant value of phase angle,  $\phi$ . Injection velocity was 20 m/s and ambient gas temperature was 3500 K.**

peak response factor was significantly greater than one, even approaching a value of eight for the 10  $\mu\text{m}$  drop size case (not shown). Calculations indicated that the peak response magnitude decreased with increasing drop size. With increasing drop size, the peak response frequency was also reduced. These results indicate the potentially dominating effects of unsteady atomization on response magnitude, and thus the growth of the instability. The effects of phase angle are important as well.

The effects of unsteady atomization and drop size on the calculated peak response magnitude are shown in Fig. 7. The phase angle,  $\phi$ , was held constant for these calculations. A comparison with the peak response magnitude calculated using continuous atomization reveals that order-of-magnitude increases in response magnitude are possible with periodic atomization. Large response magnitudes are calculated for small drops (10 and 25  $\mu\text{m}$ ) at all values of atomization frequency. For the larger drop sizes, response magnitude generally increases with decreasing atomization frequency, although peak response values remain above the continuous atomization value. The effects of periodic atomization extend further into the large drop size region as the atomization frequency is decreased.

The effects of periodic atomization on the peak response frequency are considerably less significant, as shown in Fig. 8. Again, the calculated values of peak response frequency corresponding to continuous atomization are shown for comparison. Generally, the peak response frequency calculated with periodic atomization is consistent with the calculated peak response frequency for continuous atomization, although there were some peculiar cases where significant differences occurred. These cases require further study.

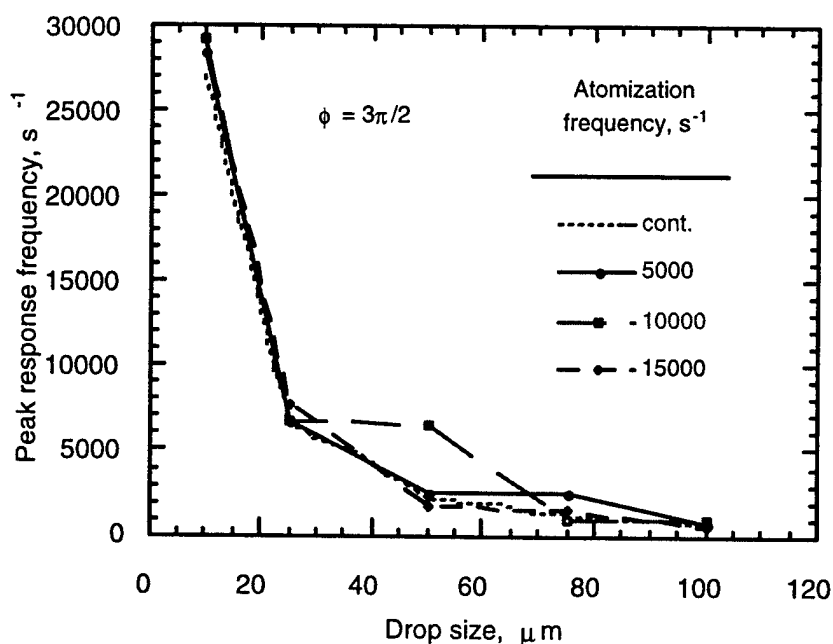


**Fig. 8.** Frequency at the peak response magnitude as a function of drop size and atomization frequency. The phase angle  $\phi$  is held constant. Injection velocity was 20 m/s and ambient gas temperature was 3500 K.

### 3.0 EXPERIMENTAL RESULTS

Experiments were conducted to determine the conditions under which periodic atomization could cause longitudinal-mode combustion instabilities in a model rocket combustor using gaseous oxygen and liquid ethanol as propellants. The experimental setup was comprised of the model rocket combustor, an impinging jet injector, piezoelectric drivers, high frequency pressure transducers, and associated flow delivery and data acquisition equipment. Additional details of the experimental setup can be found in Anderson [15].

The chamber used in the combustion modulation tests is ten inches long, and has a two-by-two inch internal cross section, as shown in Fig. 9. The frequency of the fundamental longitudinal mode of the chamber was calculated to be  $2200\text{ s}^{-1}$ , based on gas properties calculated from a one-dimensional chemical equilibrium program. The combustor was instrumented with high-frequency pressure transducers (PCB model 113A20) at approximately 0.5 inches (12.7 mm) downstream of the injection plane and at approximately 0.5 inches (12.7 mm) upstream of the nozzle throat. This allowed dynamic pressure measurements near the two pressure antinodes. The pressure transducers were calibrated *in situ*. The sensitivity of the transducer was  $2.5\text{ mV/psi}$ . ( $0.363\text{ }\mu\text{V/Pa}$ ). The signal from the high-frequency pressure transducers was sent to a data acquisition system (LeCroy model 6810) at a rate of  $50,000\text{ s}^{-1}$ , and stored on a personal computer for later analysis. The raw high frequency pressure signal

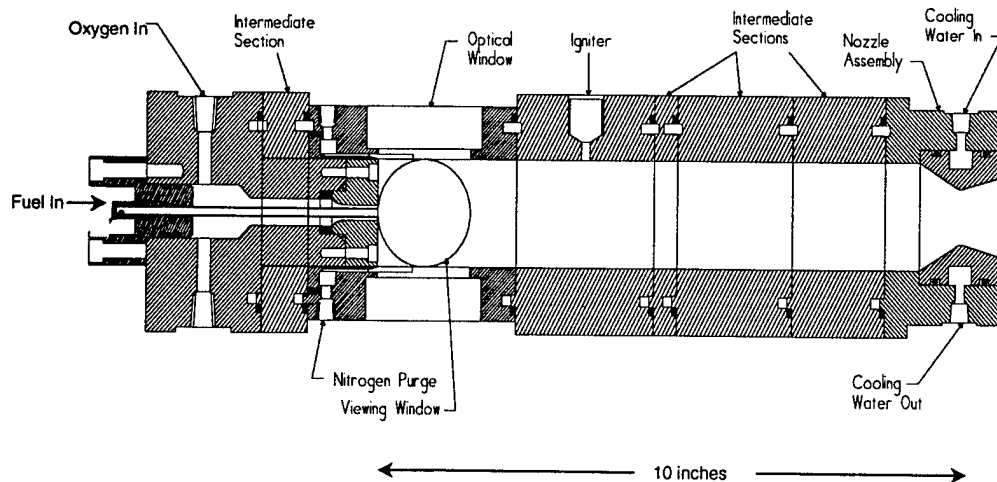


**Fig. 9. Schematic of the two-by-two inch cross-section Penn State uni-element rocket chamber. The 0.254 m (10 in) long chamber was modified to include the driven impinging jet injector system. Longitudinal combustion instabilities were driven by modulating the atomization rate of the impinging jets.**

was also sent to a fast Fourier transform spectrum analyzer (Stanford Research Systems model SR760) for real-time analysis of the power spectral density (PSD) of the chamber pressure oscillations. The PSD was monitored during the tests to evaluate the performance of the electromechanical drivers, and to guide the driver configuration.

An impinging jet injector was used, having an orifice diameter of 1.0 mm (0.040 in.) and an included impingement angle of 60°. The active injector element was based on technology developed by Dressler [16], with the basic design of the electromechanically-driven injector assembly shown in Fig. 10. The assembly, 0.152 m (6 in.) in length, is comprised of piezoelectric drivers and a nozzle holder. The driver consists of the piezoelectric transducers, a center bolt, and a piston. Fluid enters the top of the assembly and travels through the hollow center bolt to a fluid manifold, which is formed by the piston surface and an orifice plate. A voltage applied to the transducers causes the piezoelectric material to expand, and the piston is pushed toward the fixed orifice plate. As the voltage to the piezoelectric goes to zero, the center bolt provides the restoring force that draws the piston back to its original position. The voltage signals are provided to the injector system a Wavetek function generator, a Denon power amplifier, and matching transformers [16]. The function generator can supply any sort of signal form, including noise.

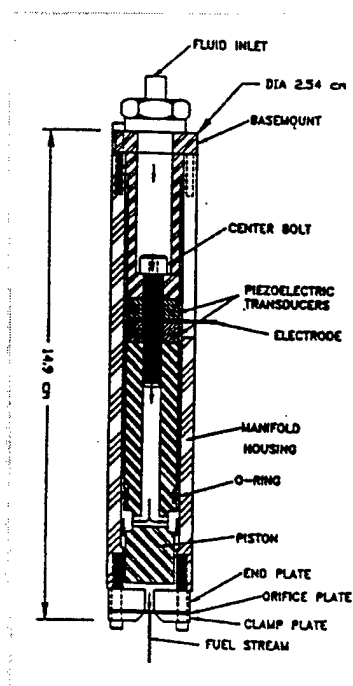


**Fig. 10. Electromechanically-driven injector assembly.**



The electromechanical drivers were incorporated into the injector such that each of the two impinging jets could be driven independently. This allowed different perturbation frequencies to be imposed on the jets, as well as variation in phase angle between the signal to each jet. Figure 11 is an image of a water spray formed by the driven impinging jet injector at atmospheric conditions. The frequency placed on each jet enhances the periodic atomization associated with the impinging jets.

The signals to the electromechanical drivers were established prior to starting the hot-fire test sequence, and left on throughout the test. The drivers were run either at the same frequency, or at different frequencies to produce a beat frequency. Drivers run at the same frequency were run either in-phase or out-of-phase with each other. In-phase driving yielded the highest pressure oscillation amplitude in the combustion tests.

The flexibility of the experimental configuration allowed the test conditions to be changed rapidly. Over 50 variations of driving conditions/flow conditions were tested. The lowest driving frequency tested was  $1800\text{ s}^{-1}$ , and the highest driving frequency tested was  $8000\text{ s}^{-1}$ . Chamber pressure and the oxidizer to fuel ratio (O/F) were held relatively constant for all tests, at about 1.448 MPa (210 psia) and 1.70, respectively. The chamber pressure was held constant for different flowrates by changing the nozzle diameter.

The frequency of the first longitudinal frequency was calculated to be about  $2200\text{ s}^{-1}$  for all conditions. The stability parameter listed in Table 2 is the value of the dimensionless



**Fig. 11. Image of spray formed by electromechanically-driven impinging injector. Jets are perturbed out-of-phase with each other at a driving frequency of  $2500\text{ s}^{-1}$ . The jet velocity is 5.2 m/s, impingement angle is 60 deg, and orifice diameter is 1.0 mm (0.04 in).**

**Table 2. Combustion Modulation Test Conditions.**

	<u>A</u>	<u>B</u>	<u>C</u>	<u>D</u>	<u>E</u>
$\dot{m}_{\text{fuel}}$ , kg/s	0.019	0.025	0.031	0.056	0.070
$\dot{m}_{\text{fuel}}$ , lb <sub>m</sub> /s	0.041	0.055	0.068	0.124	0.155
$\dot{m}_{\text{oxidizer}}$ , kg/s	0.032	0.043	0.053	0.095	0.119
$\dot{m}_{\text{oxidizer}}$ , lb <sub>m</sub> /s	0.070	0.094	0.116	0.210	0.263
$\dot{m}_{\text{coolant}}$ , kg/s	0.0068	0.0068	0.0068	0.016	0.016
$\dot{m}_{\text{coolant}}$ , lb <sub>m</sub> /s	0.015	0.015	0.015	0.035	0.035
O/F	1.70	1.71	1.71	1.69	1.69
$P_c$ , MPa	1.43	1.62	1.44	1.57	1.52
$P_c$ , psia	208	235	209	227	220
$D_{\text{throat}}$ , mm	8.76	9.55	11.3	14.6	16.6
$D_{\text{throat}}$ , in	0.345	0.376	0.443	0.575	0.652
$f$ , s <sup>-1</sup>	2200	2212	2208	2213	2212
$V_{\text{fuel}}$ , m/s	15	20	25	44	55
$p$	0.147	0.110	0.089	0.051	0.0378

parameter  $fd_o/U_j$ , where  $f$  is the pressure oscillation frequency (the first longitudinal frequency in this case),  $d_o$  is the orifice diameter, and  $U_j$  is the fuel injection velocity. The empirical stability correlation indicated that the stability parameter must be less than about 0.1 for instability to occur. Thus, Cases C, D, and E would be capable of driving an instability at the frequency of the first longitudinal mode. Case E could nearly drive a third longitudinal frequency, and this was shown to be the case.

A plot of the power spectral density (PSD) for Case E with no signal to the electromechanical drivers is shown in Fig. 12. Significant electronic noise was measured below 600 s<sup>-1</sup>. Small peaks at about 1850 s<sup>-1</sup>, 3700 s<sup>-1</sup>, and 5200 s<sup>-1</sup> were measured, corresponding to the first, second, and third longitudinal modes, respectively, and indicating a highly-damped chamber. It was found that driving the jets near the first longitudinal frequency did not produce significant levels of chamber pressure oscillations. This was primarily because of the low power output of the piezoelectric drivers at frequencies below about 4000 s<sup>-1</sup>. However, it was possible to drive significant first longitudinal pressure oscillations by causing a beat atomization

**PSD for nov14a1.e28 block 055  
no driving**

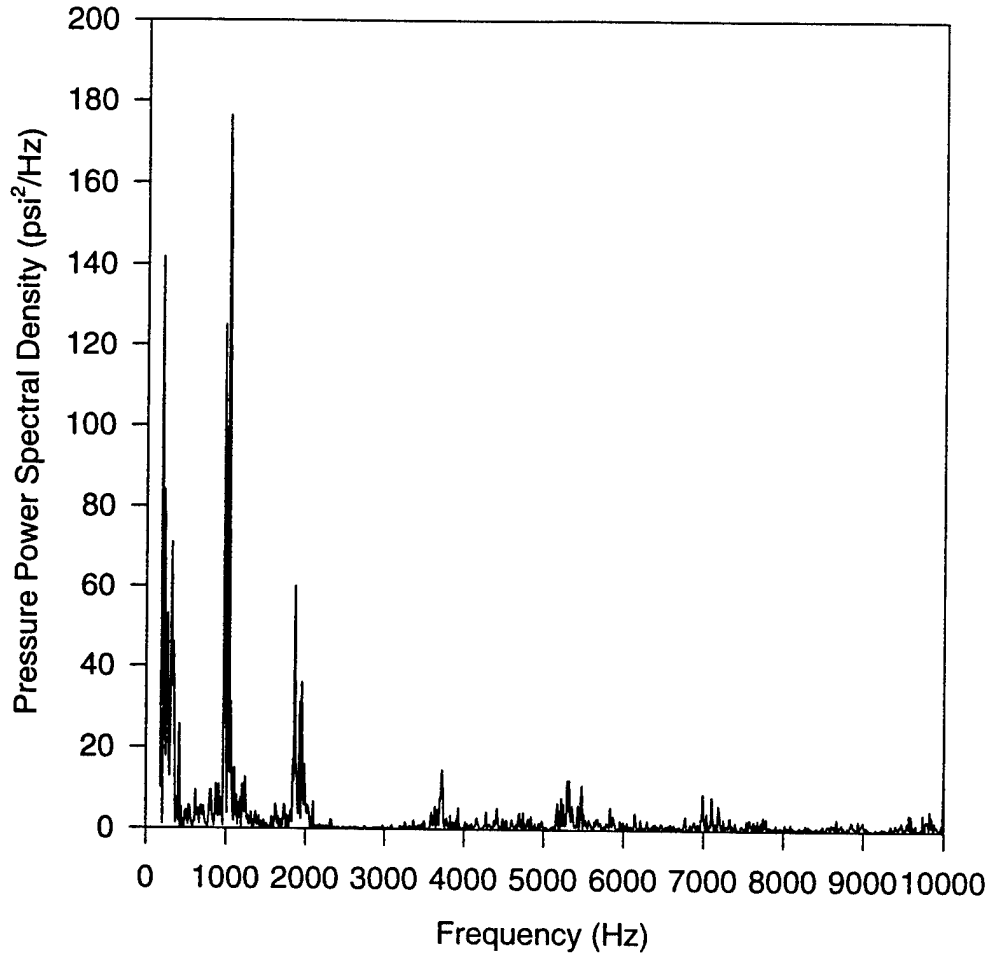


**Fig. 12. Power spectral density of pressure oscillations in 0.254 m (10 in) long chamber. Case E with no driving. Peaks corresponding to first ( $1850 \text{ s}^{-1}$ ), second ( $3700 \text{ s}^{-1}$ ) and third ( $5200 \text{ s}^{-1}$ ) longitudinal modes are shown.**

frequency near  $1900 \text{ s}^{-1}$ , as shown in Fig. 13. In this case, a  $7700 \text{ s}^{-1}$  signal was sent to one of the jets, and a  $5800 \text{ s}^{-1}$  signal was sent to the other jet to produce the beat frequency of  $1900 \text{ s}^{-1}$ .

The highest levels of pressure oscillations were achieved with high flowrates and driving frequencies of about  $5500 \text{ s}^{-1}$ , with an in-phase signal provided to the jets as shown in Fig. 14. In this case, both the first and the third longitudinal frequencies were driven. Chamber pressure time traces shown in Fig. 15 correspond to the plot of PSD shown in Fig. 14 (jets driven at  $5500 \text{ s}^{-1}$  in-phase). The oscillating chamber pressure was measured by two PCB high frequency pressure transducers, one located just downstream of the injector and the other just upstream of

**PSD for nov14a1.e32 block 064**  
 **$f_1=5800$  Hz,  $f_2=7700$  Hz,  $f_{\text{beat}}=1900$  Hz**

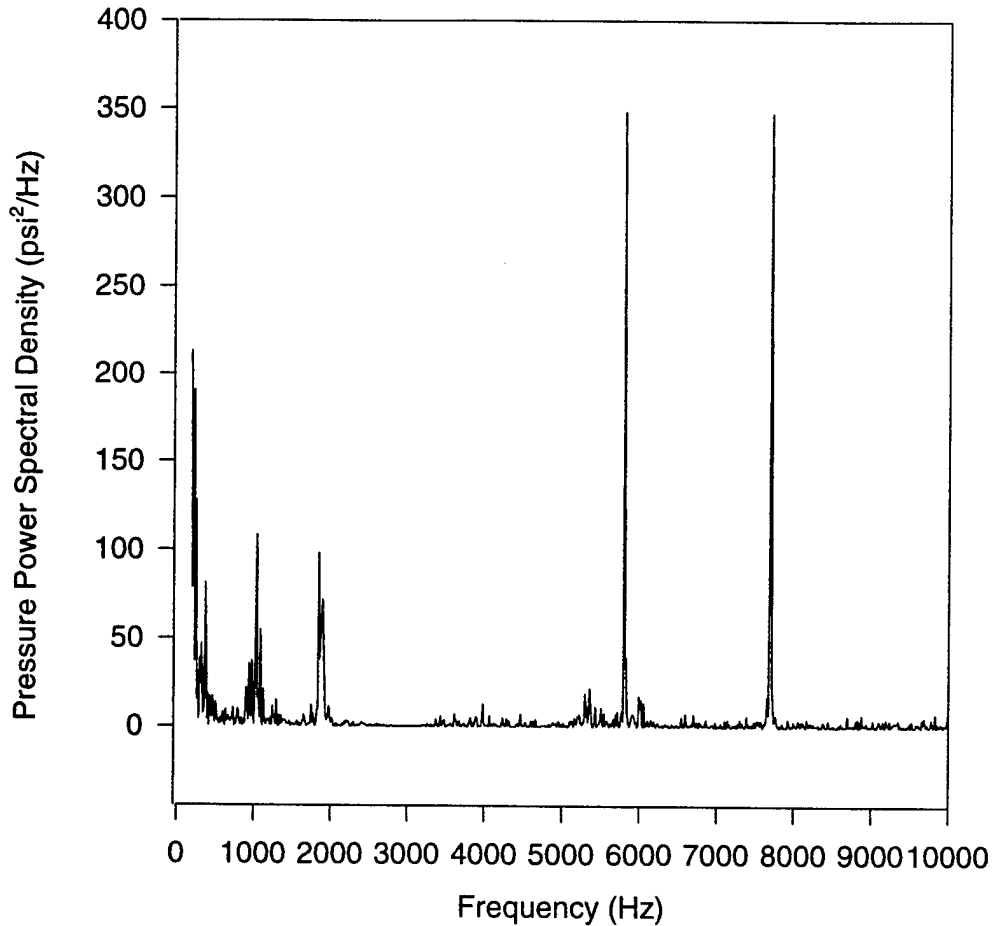


**Fig. 13. Power spectral density of pressure oscillations. Case E in which the jets are driven at  $7700\text{ s}^{-1}$  and  $5800\text{ s}^{-1}$  to produce beat frequency of  $1900\text{ s}^{-1}$ .**

the nozzle. The length of the time slice shown is  $0.005\text{ s}$ . As shown in Fig. 15, the amplitude of the pressure oscillations for the transducer just downstream of the injector is approximately  $0.138\text{ MPa}$  ( $20\text{ psi}$ ) peak-to-peak, or ten percent of the chamber pressure. For the case of no driving, the amplitude of the *unorganized* combustion noise (not shown) is about  $13.8\text{ kPa}$  (two psi) peak-to-peak, or one percent of the chamber pressure.

PSD for nov15a1.e22 block 064  
 $f_1=f_2=5500$  Hz in-phase

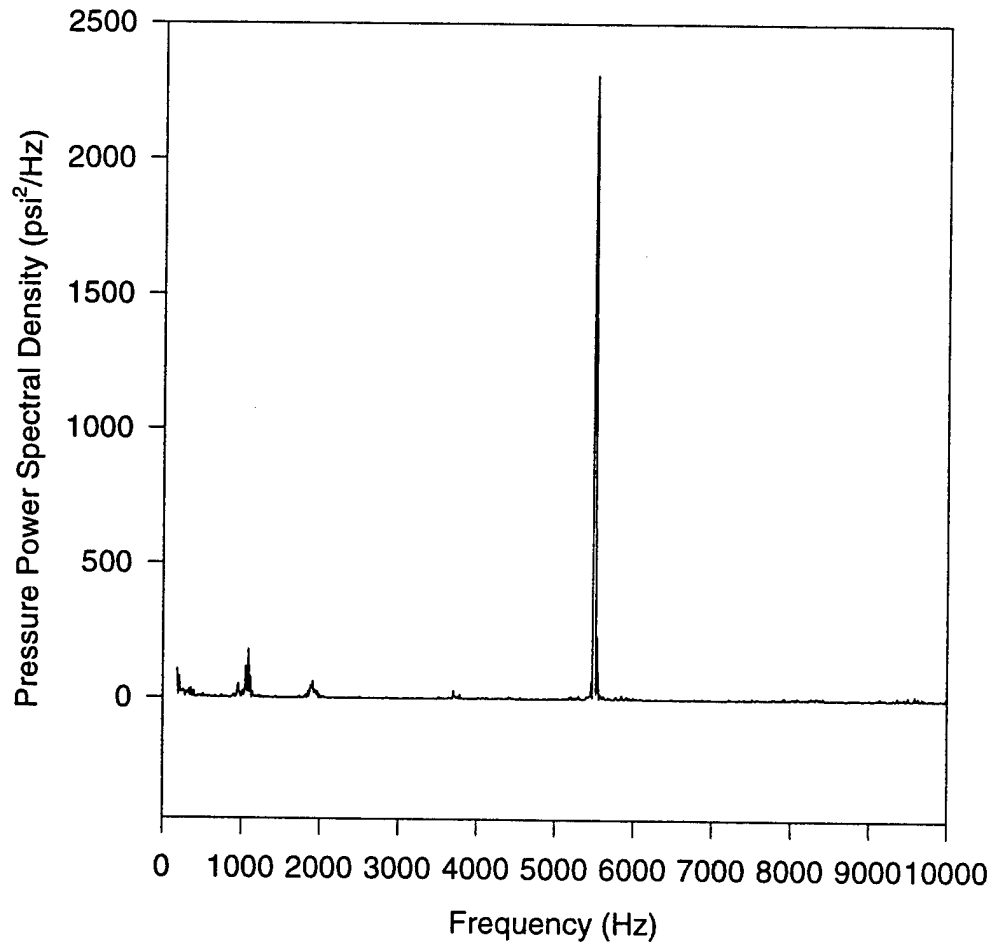


**Fig. 14.** Power spectral density of pressure oscillations. Case E in which are driven at  $5500\text{s}^{-1}$ .

### Chamber Pressure Time Trace

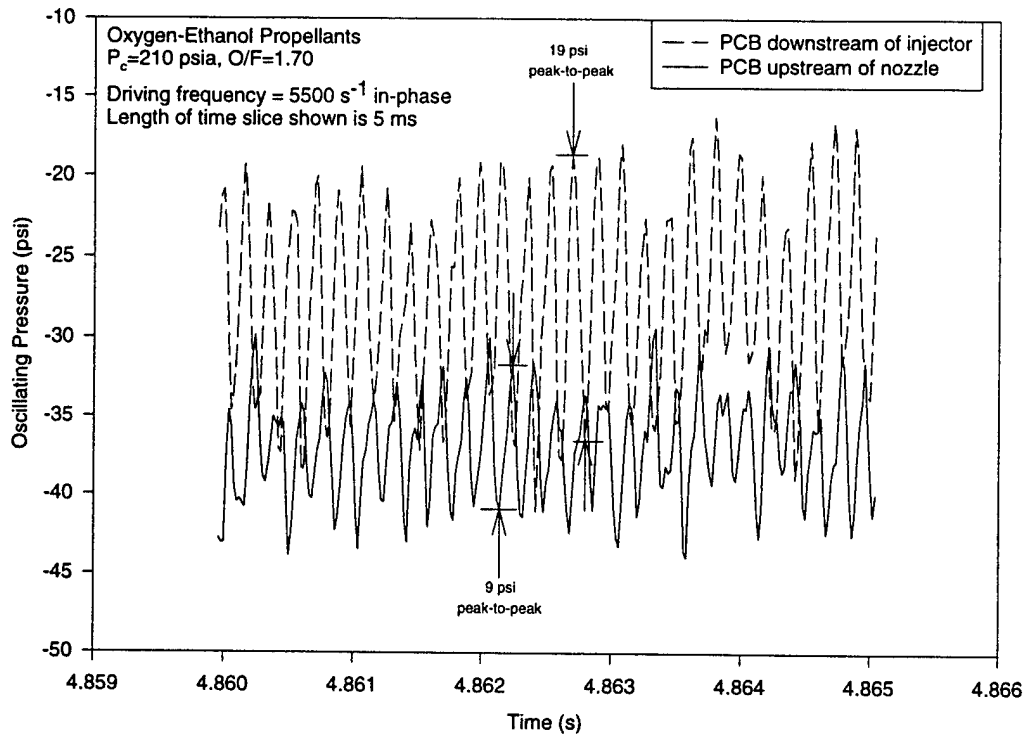


**Fig. 15.** Time traces of chamber pressure measured by high-frequency pressure transducers located just downstream of the injector and just upstream of the nozzle. The pressure trace corresponds to the PSD shown in Fig. 14 (drivers in-phase at  $5500 \text{ s}^{-1}$ ). The sampling rate is  $50,000 \text{ s}^{-1}$  and the length of the time slice shown is 0.05 s.

## 4.0 SUMMARY

To evaluate potential mechanisms of combustion instability, an analysis of the open-loop response of spray combustion to ambient acoustic oscillations was performed. The vaporization of heptane drops in an oxygen environment was considered. Combustion was assumed to occur immediately after vaporization. Experimental results provided a definition of the spray (drop size distribution, mean drop size, atomization frequency) for use as initial conditions.

When atomization occurred continuously, the results of the response analysis indicated that a wider distribution of drops reduced the response magnitude. A monodisperse size distribution gave the highest response magnitude. However, the response magnitudes for both cases were still lower than the theoretical limit necessary to drive an instability, which is consistent with most previously published results. Calculated peak response frequencies were considerably lower than the highest instability frequency predicted by an empirical stability correlation that has been proven to be accurate for combustors that use impinging jet injectors.

The major effect of including temporally-dependent atomization was a large increase in response magnitude. The response magnitude for the cases studied was far above the theoretical limit for driving an instability, and represented as much as an order of magnitude increase over the response magnitude for the continuous atomization case. Generally, the inclusion of temporally-dependent atomization did not have a major effect on the peak response frequency.

It was shown that periodic atomization can cause large variations in the response magnitude at acoustic oscillation frequencies as low as 0.1 times the atomization frequency. The increase in response magnitude was largest for small drops. The practice of using arbitrary spacing between drop injection (continuous injection or continuous atomization) yields response magnitudes that are significantly lower than are obtained with realistic atomization frequencies. Although there is evidence that oscillating ambient flowfields can significantly modify the atomization process, the precise mechanism through which coupling occurs is unknown. The analyses presented here indicated that the phase shift associated with the coupling process has an influence on both the peak response frequency and the peak response magnitude. Future work should examine the phase relationship between ambient pressure oscillations and atomization frequency.

The experimental results provide further evidence that atomization is a key mechanism in driving combustion instabilities. Pressure oscillations at frequencies corresponding to the first

through third longitudinal modes were driven in a model combustor using electromechanically-driven impinging jets. The ability to drive these very high-frequency pressure oscillations is consistent with the results from an empirical stability correlation. This experimental approach also allows, for the first time, quantitative measurements of the fundamental spray parameters that control the onset of instability.

A theory for a mechanism of combustion instability that is consistent with the results of the analytical and experimental studies presented above and the empirical stability correlation can be provided. A reduction in the value of the stability parameter ( $d_o/U_j$ ), indicating an increased tendency toward instability, implies a reduction in drop size and a reduction in the polydispersity of the spray distribution. According to the analysis presented above, however, these effects alone provide only a marginal response magnitude. An additional effect caused by a reduction in the value of the stability parameter is an increase in the atomization frequency. The large variations in response magnitude (which can be well above the theoretical limit for driving an instability) at acoustic oscillation frequencies near the atomization frequency ( $f_{osc} \sim 0.1 f_{atom}$ ) result in a large deposition of energy in a frequency-coupled resonant mode. As the stability parameter decreases, the atomization frequency increases, as does the frequency of the most energized chamber mode. The net result is an increase in the frequency range of combustion instabilities that can be driven, as indicated by the empirical stability correlation.



## 5.0 REFERENCES

- [1] *Liquid Rocket Injector Handbook*, NASA SP-8089, 1976.
- [2] Sutton, S. P., *Rocket Propulsion Elements*, 1<sup>st</sup> ed., John Wiley and Sons, New York, 1986.
- [3] Crocco, L., and Cheng, S.-I., *Theory of Combustion Instability in Liquid Propellant Rocket Motors*, AGARDograph No. 8, 1956.
- [4] Ryan, H. M., Anderson, W. E., Pal, S. and Santoro, R. J., "Atomization Characteristics of Impinging Liquid Jets," *Journal of Propulsion and Power*, Vol. 11, No. 1, pp. 135-145, 1995.
- [5] Anderson, W. E., Ryan, H.M., Santoro, R. J. and Hewitt, R.A., "Combustion Instability Mechanisms in Liquid Rocket Engines Using Impinging Jet Injectors," AIAA Paper No. 95-2357, 31st AIAA/ASME/SAE/ASEE Joint Propulsion Conference and Exhibit, San Diego, CA, July 10-12, 1995.
- [6] Anderson, W. E., and Santoro, R. J., "The Effects of Drop Size Distribution and Atomization Periodicity on Combustion Response," AIAA Paper No. 96-3027, 32nd AIAA/ASME/SAE/ASEE Joint Propulsion Conference and Exhibit, Lake Buena Vista, FL, July 1-3, 1996.
- [7] Heidmann, M. F. and Wieber, P. R., "An Analysis of the Frequency Response Characteristics of Propellant Vaporization," NASA TN D-3749, 1966.
- [8] Priem, R. J. and Heidmann, M. F., "Propellant Vaporization as a Design Criterion for Rocket Engine Combustion Chambers," NASA TR R-67, 1960.
- [9] Tong, A.-Y. and Sirignano, W. A., "Oscillatory Vaporization of Fuel Droplets in an Unstable Combustor", *J. Propulsion*, Vol. 5, No. 3, pp. 257-261, 1989.
- [10] Anderson, W. E., Ryan, H. M. and Santoro, R. J., "A Model for Impinging Jet Injector Atomization," 32nd JANNAF Combustion Subcommittee Meeting and Propulsion Engineering Research Center 7th Annual Symposium, CPIA Publication 631, Vol. II, pp. 55-64, 1995.
- [11] Dombrowski, N. and Hooper, P. C., "The Performance Characteristics of an Impinging Jet Atomizer in Atmospheres of High Ambient Density," *Fuel*, pp. 323-334, 1962.
- [12] Priem, R. J. and Guentert, D. C., "Combustion Instability Limits Determined by a Nonlinear Theory and a One-Dimensional Model," NASA TN D-1409, 1962.

- [13] Muss, J. A., Nguyen, T.-V. and Johnson, C. W., *User's Manual for Rocket Combustor Interactive Design (ROCCID) and Analysis Computer Program*, NASA CR 187110, 1991.
- [14] Strahle, W. C. and Crocco, L., Analytical Investigation of Several Mechanisms of Combustion Instability, Bulletin of the 5th Liquid Propulsion Symposium, CPIA Publication No. 34, Vol. 2, 1963.
- [15] Anderson, W. E., "Demonstration of Combustion Modulation Techniques for Active Control of High-Energy-Density Propellant Combustion in Rocket Engines," Final Report, Contract NAS8-40626, George C. Marshall Space Flight Center, Huntsville, AL., 1996.
- [16] Dressler, J. L., "Two-Dimensional, High-Flow, Precisely Controlled Monodisperse Drop Source," Final Report, WL/TR-93-2049, Aero Propulsion and Power Directorate, Wright Laboratory, Air Force Materiel Command, Wright-Patterson AFB OH, 1993.

## 6.0 PUBLICATIONS

Ryan, H. M., Anderson, W. E., Pal, S. and Santoro, R. J., "Atomization Characteristics of Impinging Liquid Jets," *Journal of Propulsion and Power*, Vol. 11, No. 1, pp. 135-145, 1995.

Anderson, W. E., Ryan, H.M., Santoro, R. J. and Hewitt, R.A., "Combustion Instability Mechanisms in Liquid Rocket Engines Using Impinging Jet Injectors," AIAA Paper No. 95-2357, 31st AIAA/ASME/SAE/ASEE Joint Propulsion Conference and Exhibit, San Diego, CA, July 10-12, 1995.

Anderson, W. E., and Santoro, R. J., "The Effects of Drop Size Distribution and Atomization Periodicity on Combustion Response," AIAA Paper No. 96-3027, 32nd AIAA/ASME/SAE/ASEE Joint Propulsion Conference and Exhibit, Lake Buena Vista, FL, July 1-3, 1996.

Anderson, W. E., Ryan, H. M. and Santoro, R. J., "A Model for Impinging Jet Injector Atomization," 32nd JANNAF Combustion Subcommittee Meeting and Propulsion Engineering Research Center 7th Annual Symposium, CPIA Publication 631, Vol. II, pp. 55-64, 1995.

Anderson, W. E., Miller, K. L., Ryan, H. M., Pal, S., Santoro, R. J. and Dressler, J. L., "The Effects of Periodic Atomization on Combustion Instability in Liquid-Fueled Primary Stage Propulsion Systems," to be submitted to *Journal of Propulsion and Power*.

Rahman, S., Cramer, J., Pal, S. and Santoro, R. J., "Coaxial Swirl Injector Studies at High O/F Ratios," JANNAF CS/PSH/EPTS/SPIRITS Joint Meeting, Huntsville, AL, October 23-27, 1995.

Pal, S., Moser, M. D., Ryan, H. M., Foust, M. J. and Santoro, R. J., "Shear Coaxial Injector Atomization Phenomena for Combusting and Non-Combusting Conditions," *Atomization and Sprays*, Vol. 6, 1996, pp. 227-244.

Rahman, S. A., Pal, S. and Santoro, R. J., "Swirl Coaxial Atomization; Cold Flow and Hot-Fire Experiments," AIAA Paper No. 95-0381, 33rd AIAA AeroSpace Sciences Meeting, Reno, NV, January 9-12, 1995.

Anderson, W. E. and Dressler, J. L., "Demonstration of Spray Modulation Techniques for control of Combustion Instabilities in Rocket Engines," 10<sup>th</sup> Annual Conference on Liquid Atomization and Spray Systems (ILASS), Ottawa, ON, Canada, May 18-21, 1997, pp.220-224.

Rahman, S. A. and Santoro, R. J., "A Review of Coaxial Gas/Liquid Spray Experiments and Correlations," AIAA Paper No. 94-2772, 30th AIAA/ASME/SAE/ASEE Joint Propulsion Conference, Indianapolis, IN, June 27-29, 1994.

## **7.0 PARTICIPATING PROFESSIONALS**

Prof. Robert J. Santoro, Professor of Mechanical Engineering, Co-Principal Investigator

Dr. William E. Anderson, Associate Director of PERC, Co-Principal Investigator

Dr. Sibtosht Pal, Senior Research Associate, Mechanical Engineering Department

Dr. Harry M. Ryan, Graduate Student, Ph.D from Mechanical Engineering Department (1994)

Ms. Kristin Miller, Graduate Student, Mechanical Engineering Department (Expected MS, 1998)

Mr. Larry Schaaf, Senior Research Technician, Mechanical Engineering Department

## 8.0 MEETINGS AND PRESENTATIONS

Anderson, W. E., Ryan, H.M., Santoro, R. J. and Hewitt, R.A., "Combustion Instability Mechanisms in Liquid Rocket Engines Using Impinging Jet Injectors," 31st AIAA/ASME/SAE/ASEE Joint Propulsion Conference and Exhibit, San Diego, CA, July 10-12, 1995.

Anderson, W. E., and Santoro, R. J., "The Effects of Drop Size Distribution and Atomization Periodicity on Combustion Response," 32nd AIAA/ASME/SAE/ASEE Joint Propulsion Conference and Exhibit, Lake Buena Vista, FL, July 1-3, 1996.

Anderson, W. E., Ryan, H. M. and Santoro, R. J., "A Model for Impinging Jet Injector Atomization," 32nd JANNAF Combustion Subcommittee Meeting and Propulsion Engineering Research Center 7th Annual Symposium, 1995.

Rahman, S., Cramer, J., Pal, S. and Santoro, R. J., "Coaxial Swirl Injector Studies at High O/F Ratios," JANNAF CS/PSH/EPTS/SPIRITS Joint Meeting, Huntsville, AL, October 23-27, 1995.

Rahman, S. A., Pal, S. and Santoro, R. J., "Swirl Coaxial Atomization; Cold Flow and Hot-Fire Experiments," 33rd AIAA AeroSpace Sciences Meeting, Reno, NV, January 9-12, 1995.

Anderson, W. E. and Dressler, J. L., "Demonstration of Spray Modulation Techniques for control of Combustion Instabilities in Rocket Engines," 10<sup>th</sup> Annual Conference on Liquid Atomization and Spray Systems (ILASS), Ottawa, ON, Canada, May 18-21, 1997.

Rahman, S. A. and Santoro, R. J., "A Review of Coaxial Gas/Liquid Spray Experiments and Correlations," 30th AIAA/ASME/SAE/ASEE Joint Propulsion Conference, Indianapolis, IN, June 27-29, 1994.

Anderson, W. E. and Santoro, R. J., "The Role of Unsteady Atomization in Combustion Instability," Propulsion Engineering Research Center, Penn State, Eight Annual Symposium, The Pennsylvania State University, October 30-31, 1996, University Park, PA.

## **9.0 INTERACTIONS**

The design/experimental phase of the combustion experiments described in this final report involved extensive interactions with Dr. John Dressler of Fluid Jet Associates. Specifically, the oscillatory flow experiments involving the piezo-electric drivers for impinging jet injectors required close cooperation between the experimentalists at Penn State and Dr. Dressler.